**Electronic Supplementary Information†**

# Solubility and permeability enhancement of BCS class IV drug Ribociclib through cocrystallization

*M. K. Chaitanya Mannava,[a], Abhijit Garai,[a] Manish K. Bommaka,[a] K. Anand Solomon,[b]* and Ashwini K. Nangia[a]**

[a] School of Chemistry, University of Hyderabad, Central University P.O., Prof. C. R. Rao Road, Hyderabad 500046, India.

[b] Department of Chemistry, School of Engineering, Dayananda Sagar University, Kudlu Gate, Bangalore 560068, India

Correspondence email: ashwini.nangia@gmail.com, anands-chem@dsu.edu.in

**Contents:**

## 1. Infrared (IR) Spectroscopy

FT-IR spectroscopy is useful to understand the formation of cocrystal or salt and the presence of hydrogen bonds (peaks are listed in Table S1 and Fig. S1-S3. In RBC-RES complex, the C=O stretching frequency of CONMe2 group is slightly red-shifted due to hydrogen bonding with OH of RES. Stretching frequency of OH and NH are shifted and the peaks are broader due to hydrogen bonding. In case of RBC-VA complex, the C=O stretching frequency of VA is significantly red-shifted from 1682 $cm^{-1}$ to 1600 $cm^{-1}$, a clear indication of carboxylate anion from neutral COOH. Peaks of OH and NH stretching frequency are red-shifted and broadened in the hydrogen-bonded adducts.

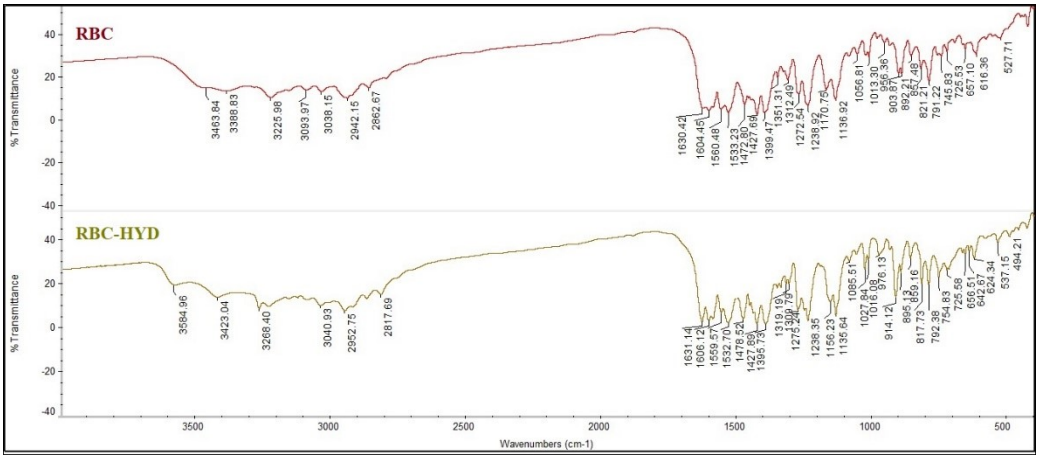


**Fig. S1** IR spectra of RBC-HYD compared with the starting material RBC.

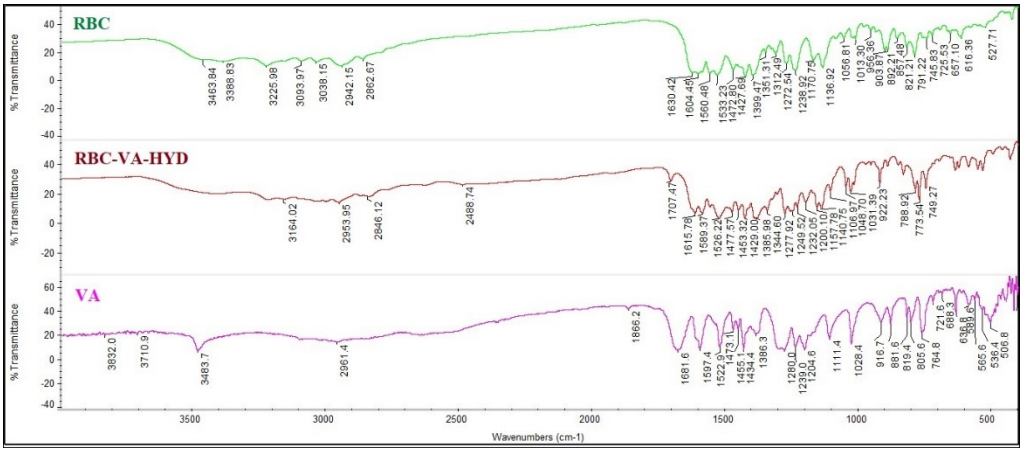


**Fig. S2** IR spectra of RBC-VA-HYD compared with the starting material RBC and the coformer VA.

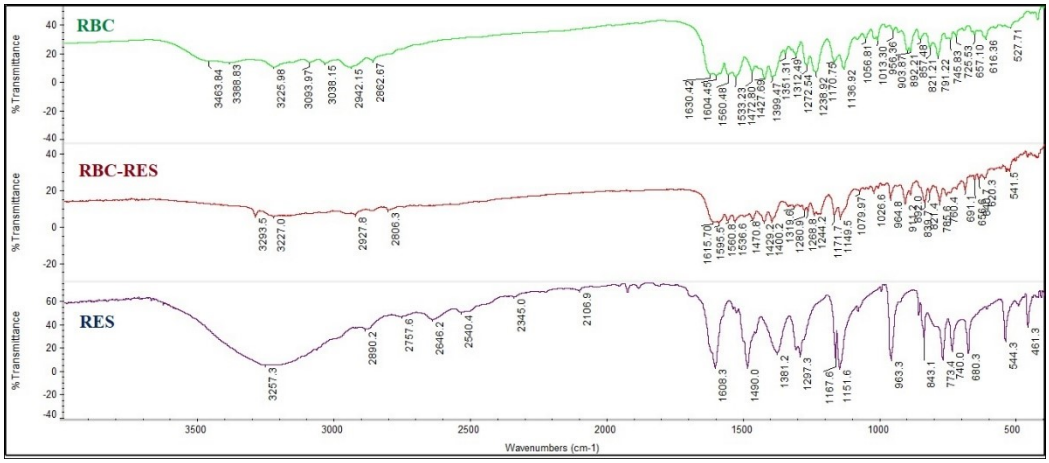


**Fig. S3** IR spectra of RBC-RES compared with the starting material RBC and the coformer RES.

**Table S1** FT-IR stretching frequency for COOH, COO-, NH/OH and aliphatic and aromatic CH peaks of RBC and coformers.

| Compound | $\nu_{C=O}$ ($cm^{-1}$) for -COOH/ -COO-/ $-CONMe_2$ | $\nu_{N-H/O-H}$ ($cm^{-1}$) | $\nu_{C-H}$ ($cm^{-1}$) for aliphatic and aromatic CH |
|---|---|---|---|
| RBC | 1630, 1604 | 3464, 3389, 3226 | 3094, 3038, 2942, 2863 |
| RBC-HYD | 1631, 1606 | 3585, 3423, 3268 | 3041, 2953, 2818 |
| RES | --- | 3257 | 2890, 2758 |
| RBC-RES | 1616, 1596 | 3294, 3227 | 2928, 2806 |
| VA | 1682 | 3484 | 2961 |
| RBC-VA-HYD | 1616, 1589 | 3400-3500 (broad), 3164 | 2954, 2846 |

## 2. PXRD for bulk-phase purity

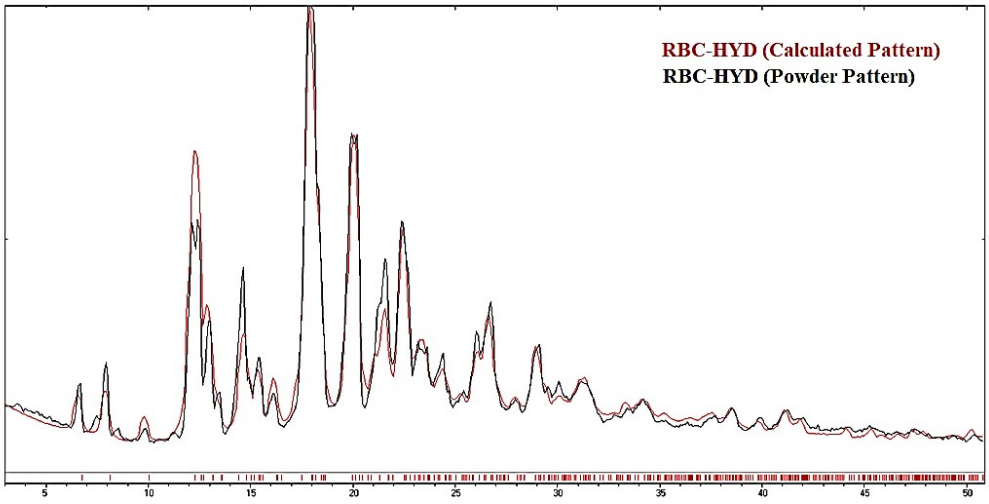


(a)

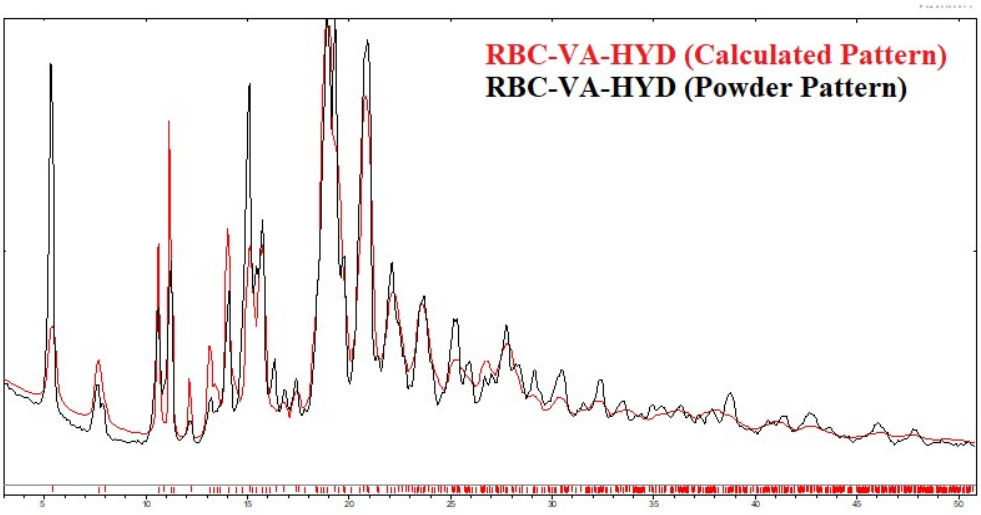


(b)

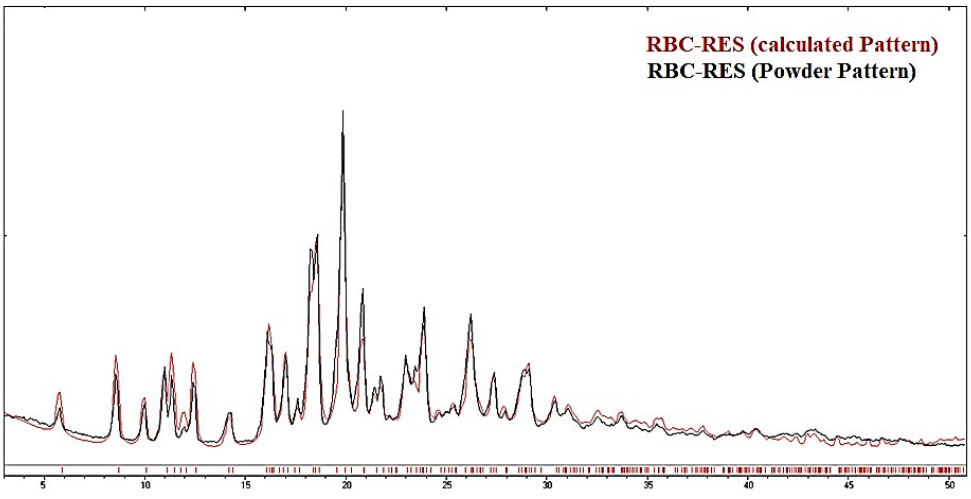

(c)

**Fig. S4** (a) The experimental PXRD pattern of RBC-HYD (b) multicomponent solids (RBC-VA-HYD) and (c) RBC-RES, (black) matches with the calculated line profile from the calculated X-ray crystal structure (red), indicating bulk purity and phase homogeneity. Rietveld refinement for RBC-HYD gave $R_p$ = 0.1127, $R_{wp}$ = 0.1506, $R_{exp}$ = 0.1082; RBC-VA-HYD gave $R_p$ = 0.3254, $R_{wp}$ = 0.4650, $R_{exp}$ = 0.8823; and for RBC-RES gave $R_p$ = 0.1259, $R_{wp}$ = 0.1670, $R_{exp}$ = 0.7349.

The crystalline phase of RBC-HYD after heating and loss of water was confirmed to be the same as that of RBC (anhydrous) by using a combination of heat-cool cycle in TGA and then PXRD on the sample after cooling.

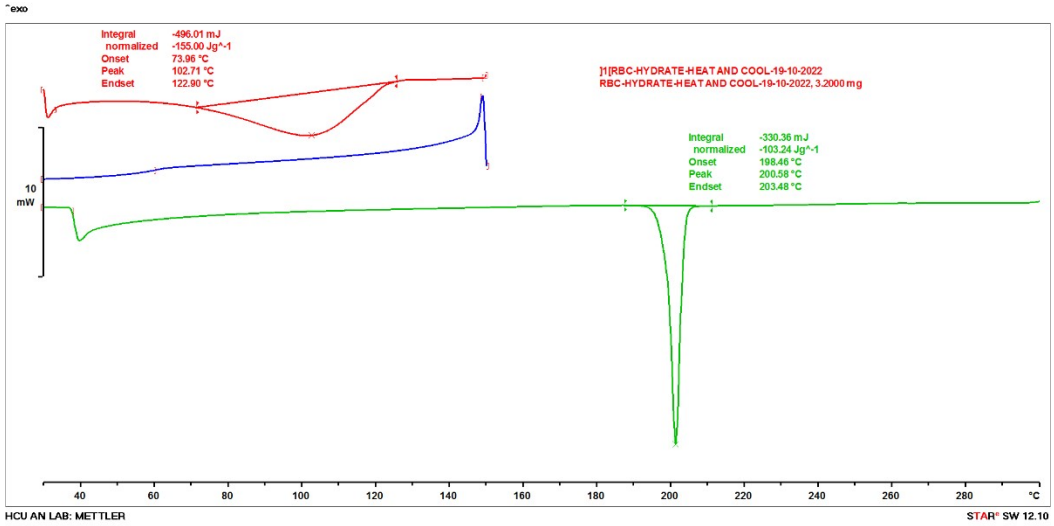


**Fig. S5.** Fresh sample of RBC after dehydration was prepared in DSC-TGA instrument after heating to 155 °C past the dehydration endotherm for water loss, then cooled to 40 °C and then re-heated to observe a DSC endotherm at the temperature matching with the melting of pure RBC (201-202 °C).

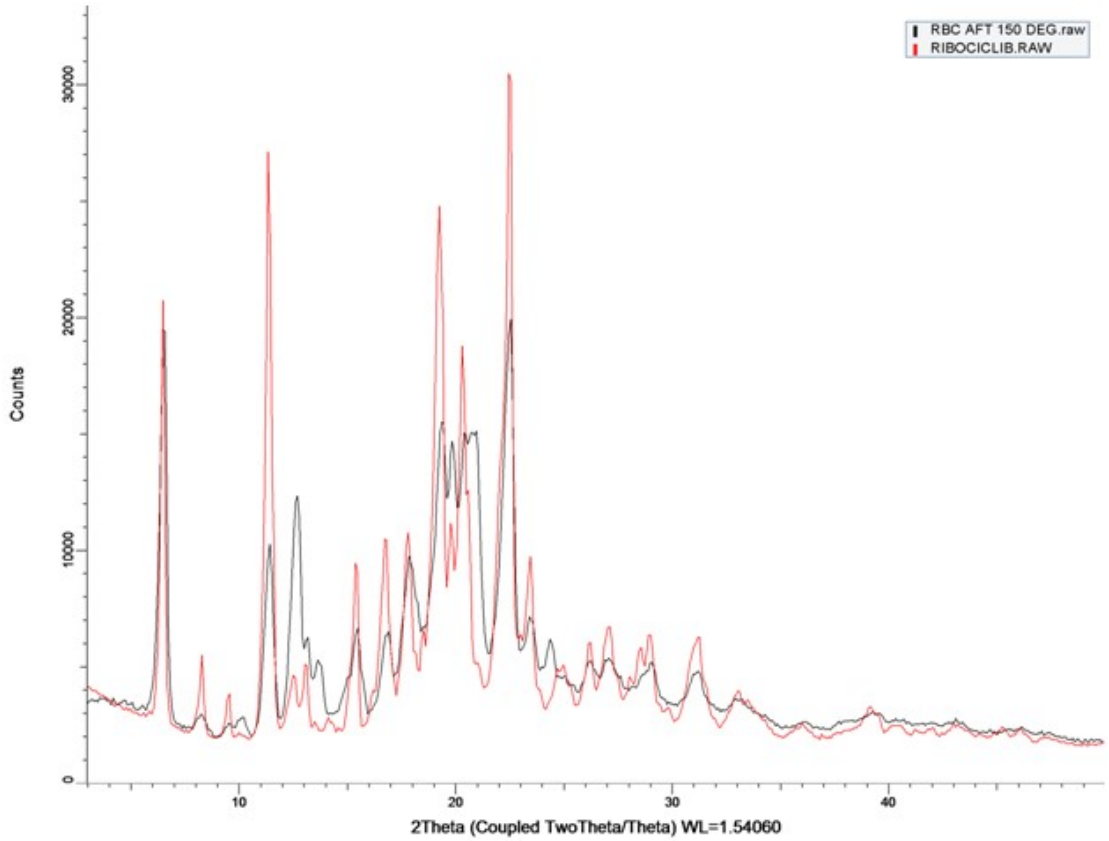


**Fig. S6** PXRD on the cooled solid was recorded to confirm that the RBC-HYD sample after heat-cool cycle matches with that of reference RBC.

**3. PXRD after equilibrium solubility and IDR experiments**

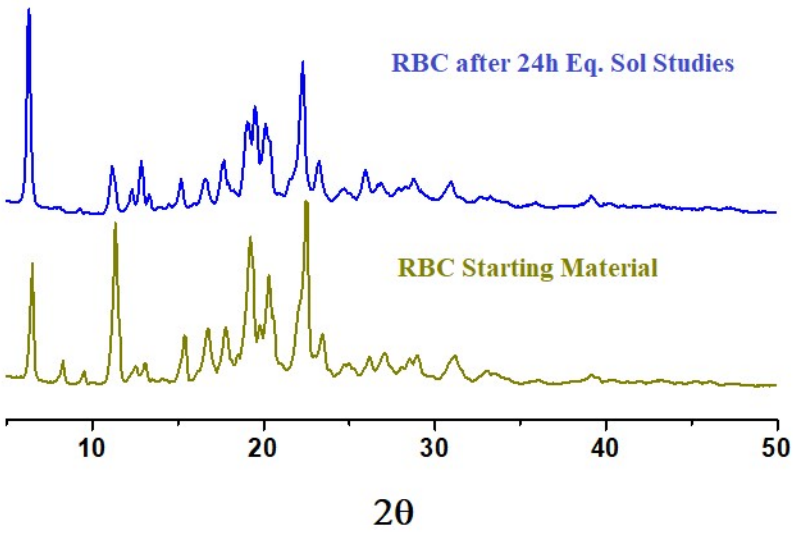


**Fig. S7** PXRD of RBC at the end of equilibrium solubility experiment (24 h, blue) matches with the initial PXRD pattern of RBC (green) indicating stable.

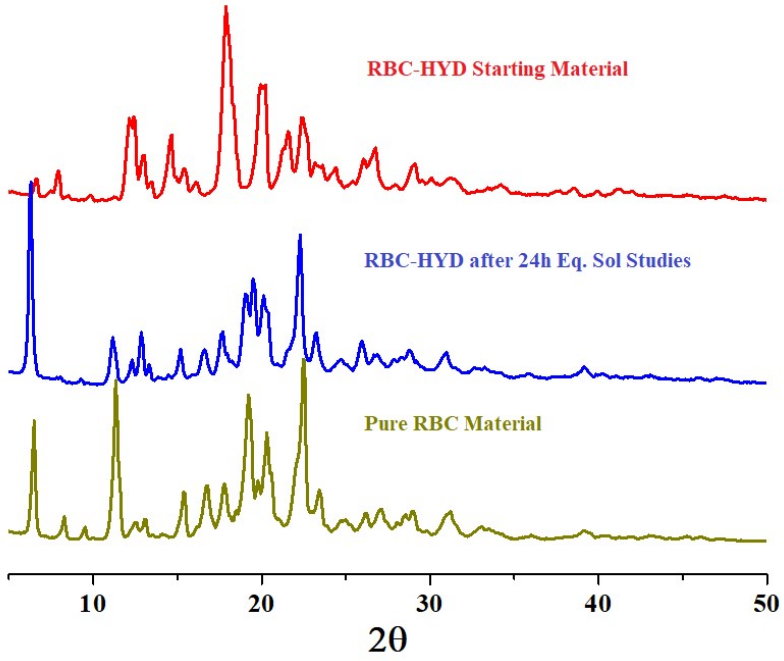


**Fig. S8** PXRD of RBC-HYD at the end of equilibrium solubility experiment (24 h, blue) does not match with the initial PXRD pattern of RBC-HYD (red) but the diffraction lines overlay with that of pure RBC (green) indicating unstable form.

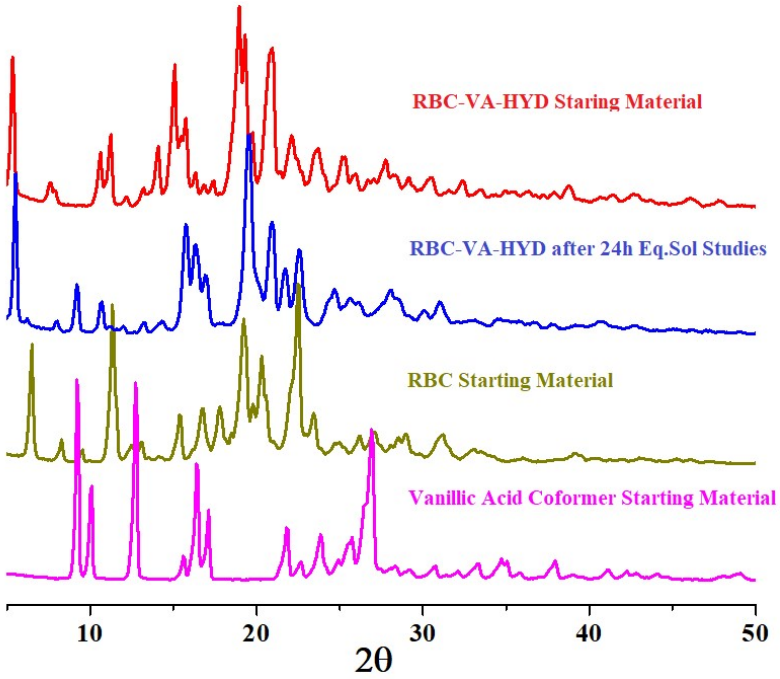


**Fig. S9** PXRD of RBC-VA-HYD salt at the end of equilibrium solubility experiment (24 h, blue) does not match with the initial PXRD pattern of RBC-VA-HYD (red) but the diffraction lines overlay with that of pure RBC (green) and the coformer vanillic acid indicating dissociation of the salt to the drug.

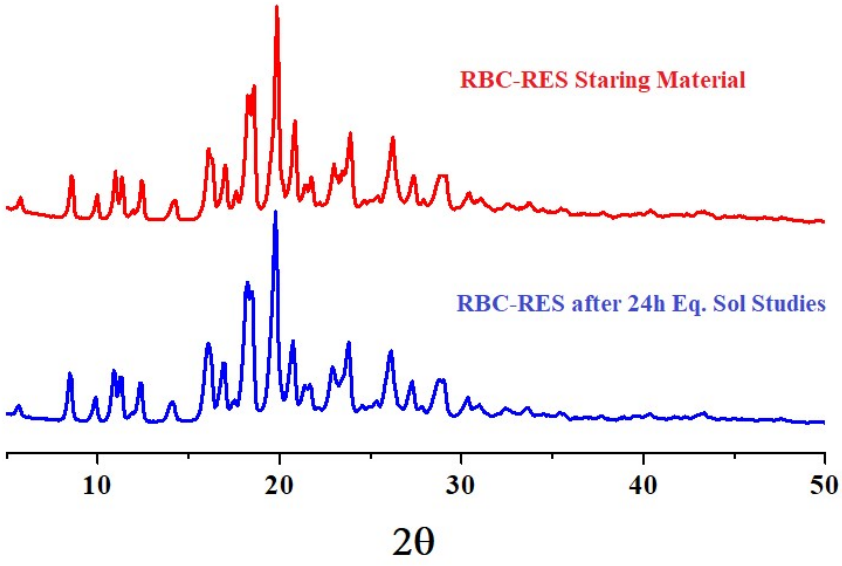


**Fig. S10** PXRD of RBC-RES cocrystal at the end of equilibrium solubility experiment (24 h, blue) matches with the initial PXRD pattern of RBC-RES (red) indicating phase stability.

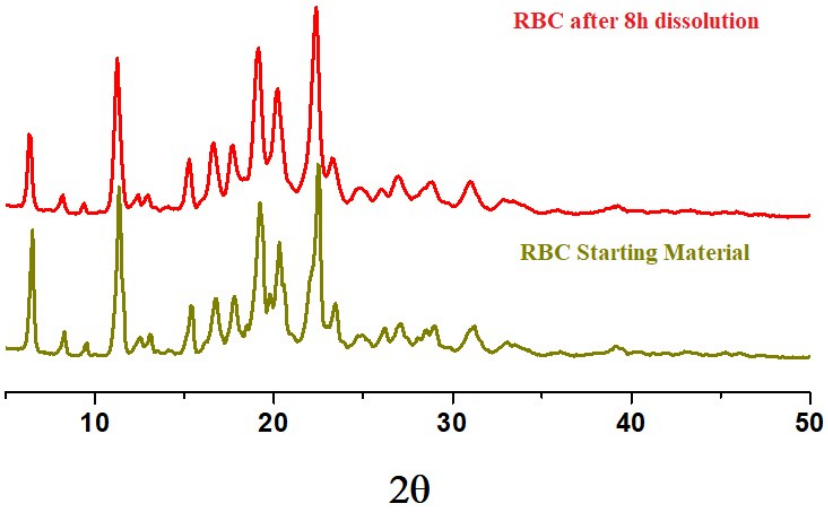


**Fig. S11** PXRD of RBC at the end of intrinsic dissolution rate experiment (8 h, red) matches with the initial PXRD pattern of RBC (green) indicating stable form.

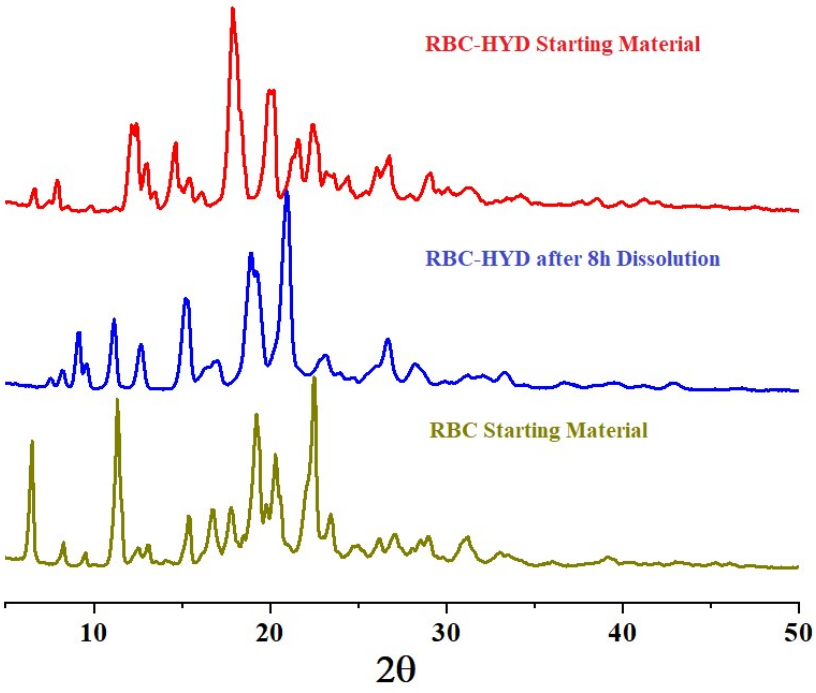


**Fig. S12** PXRD of RBC-HYD at the end of intrinsic dissolution rate experiment (8 h, blue) does not match with the initial PXRD pattern of RBC-HYD (red) but the diffraction lines overlay with that of pure RBC (green) indicating unstable form.

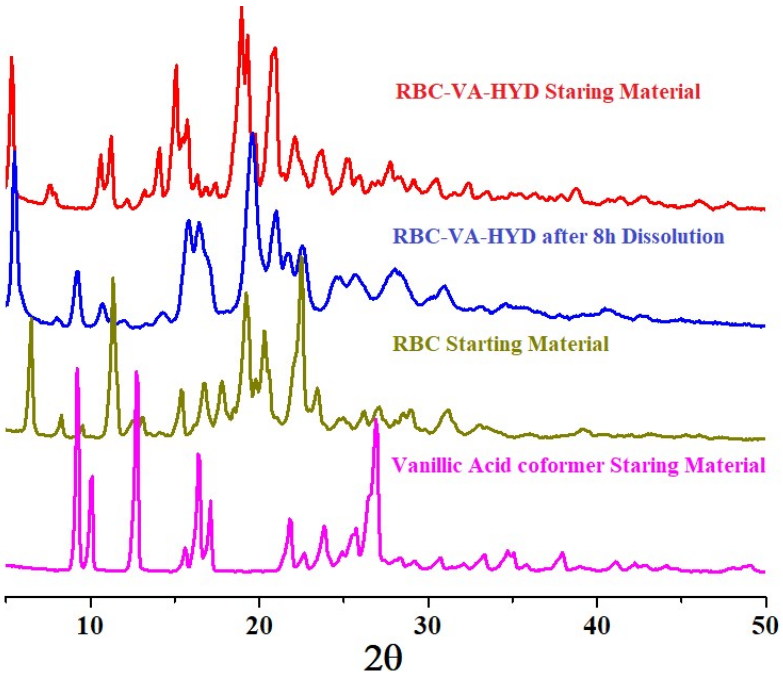

**Fig. S13** PXRD of RBC-VA-HYD salt at the end of intrinsic dissolution rate experiment (8 h, blue) does not match with the initial PXRD pattern of RBC-VA-HYD (red) but the diffraction lines overlay with that of pure RBC (green) and the coformer vanillic acid indicating dissociation of the salt to the drug.

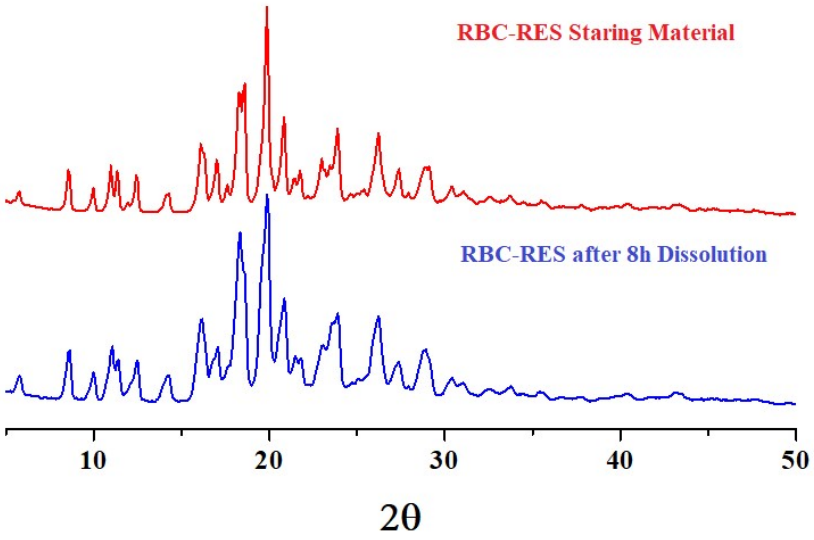


**Fig. S14** PXRD of RBC-RES cocrystal at the end of intrinsic dissolution rate experiment (8 h, blue) matches with the initial PXRD pattern of RBC-RES (red) indicating phase stability.

## 4. Crystallographic and hydrogen bond parameters

**Table S2** Crystallographic parameters of RBC-HYD, RBC-VA-HYD and RBC-RES.

| Compound | RBC-HYD | RBC-VA-HYD | RBC-RES |
|---|---|---|---|
| Emp. formula | $C_{23}H_{30}N_8O$, $H_2O$ | $C_{23}H_{31}N_8O$, $C_8H_7O_4$, $H_2O$ | $C_{23}H_{30}N_8O$, $C_6H_6O_2$ |
| Formula wt. | 452.56 | 620.71 | 544.66 |
| Cryst. System | monoclinic | monoclinic | monoclinic |
| Space group | $P2_1/n$ | $P2_1/n$ | $P2_1/c$ |
| T (K) | 293(2) | 293(2) | 293(2) |
| *a* (Å) | 7.5763(6) | 11.9881(8) | 8.5570(6) |
| *b* (Å) | 25.947(2) | 8.0148(5) | 29.967(2) |

| | | | |
|---|---|---|---|
| *c* (Å) | 12.1602(10) | 32.4063(19) | 11.5654(9) |
| α (deg) | 90 | 90 | 90 |
| β (deg) | 100.659(4) | 93.301(2) | 111.625(2) |
| γ (deg) | 90 | 90 | 90 |
| Z | 4 | 4 | 4 |
| V (Å$^3$) | 2349.2(3) | 3108.5(3) | 2756.9(4) |
| Unique rflns | 3024 | 5123 | 3522 |
| Obsd rflns | 4898 | 7160 | 8212 |
| Parameters | 307 | 413 | 375 |
| $R_1$ | 0.0734 | 0.0667 | 0.0733 |
| $wR_2$ | 0.2192 | 0.1922 | 0.2015 |
| GOF | 1.065 | 0.991 | 1.016 |
| Diffractometer | Bruker | Bruker | Bruker |

**Table S3** Hydrogen bond parameters in RBC-HYD, RBC-VA-HYD and RBC-RES.

| D–H···A | D···A /Å | H···A /Å | D–H···A /° | symmetry code |
|---|---|---|---|---|
| RBC-HYD | | | | |
| N5-H5N···N6 | 3.070(3) | 2.23 | 165 | -x,1-y,2-z |
| O1W-H1WA···N8 | 2.842(6) | 2.03 | 160 | 3/2-x,-1/2+y,3/2-z |
| O1W-H1WB···O1 | 2.693(5) | 1.87 | 164 | x,y,z |
| N8-H8N···N4 | 3.322(4) | 2.59 | 160 | 1-x,1-y,2-z |
| C19-H19···N4 | 3.299(4) | 2.54 | 139 | -x,1-y,2-z |
| C5-H5···O1W | 3.263(6) | 2.44 | 148 | -1+x,y,z |
| C16-H16···N3 | 2.907(4) | 2.31 | 122 | Intra |
| C3-H3A···O1W | 3.254(8) | 2.36 | 155 | -1+x,y,z |
| C2-H2C···O1 | 2.678(6) | 2.30 | 102 | Intra |
| RBC-VA-HYD | | | | |
| O5-H5O···O2 | 2.662(3) | 1.86 | 167 | 3/2-x,-1/2+y,1/2-z |
| N8-H8B···O3 | 2.847(3) | 2.05 | 149 | 1/2-x,-1/2+y,1/2-z |
| N5-H5N···N6 | 3.194(2) | 2.34 | 171 | 1-x,-y,1-z |
| N8-H8A···O3 | 2.755(3) | 1.89 | 163 | x,-1+y,z |
| O1W-H1WB···O2 | 2.822(3) | 1.98 | 170 | x,-1+y,z |
| O1W-H1WA···O1 | 2.930(3) | 2.09 | 170 | -1/2+x,3/2-y,-1/2+z |
| C23-H23A···O1 | 3.412(3) | 2.59 | 142 | 1-x,1-y,1-z |
| C5-H5···O2 | 3.334(3) | 2.47 | 155 | 1/2+x,3/2-y,1/2+z |

| | | | | |
|---|---|---|---|---|
| C16-H16···N3 | 2.921(3) | 2.33 | 122 | Intra |
| C12-H12A···N4 | 3.519(6) | 2.58 | 162 | x,1+y,z |
| RBC-RES | | | | |
| N8-H8N···O2 | 3.080(4) | 2.22 | 151 | 1-x,1/2+y,1/2-z |
| O2-H2O···O1 | 2.651(3) | 1.87 | 159 | x,y,z |
| O3-H3O···N8 | 2.767(4) | 1.97 | 165 | -x,1-y,-z |
| N5-H5N···N4 | 3.092(3) | 2.34 | 168 | 2-x,1-y,-z |
| C16-H16···N3 | 2.929(3) | 2.34 | 121 | Intra |
| C2-H2C···O1 | 2.699(4) | 2.31 | 104 | Intra |
| C12-H12A···N3 | 3.222(4) | 2.57 | 125 | Intra |

**5. Equilibrium solubility, IDR and diffusion data**

**Table S4** Equilibrium solubility and IDR of RBC, RBC-HYD, RBC-VA-HYD and RBC-RES.

| API/Coformer | Solubility of API/coformer in water (mg. $mL^{-1}$) | Compound | Equilibrium solubility of API/ salt/ cocrystal in PBS media | Intrinsic dissolution rate, IDR, mg. $cm^{-2}.min^{-1}$ |
|---|---|---|---|---|
| **RBC** | 0.24 | RBC | 0.21 | 0.07 |
| | | RBC-HYD (1:1) | 0.26 | 0.08 |
| **VA** | 18.6 | RBC-VA-HYD (1:1:1) | 0.36 | 0.16 |
| **RES** | 82.3 | RBC-RES (1:1) | 0.44 | 0.10 |

**Table S5** Cumulative Amount dissolved at different time intervals for RBC, RBC-HYD, RBC-VA-HYD and RBC-RES.

| | Cumulative Amount dissolved (mg/500 mL) | | | |
|---|---|---|---|---|
| Time Intervals (min) | RBC | RBC-HYD | RBC-RES | RBC-VA-HYD |
| 0 | 0 | 0 | 0 | 0 |
| 15 | 1.5269 | 1.5619 | 1.9973 | 5.5109 |
| 30 | 3.6112 | 2.6877 | 3.5179 | 8.7356 |
| 60 | 6.1198 | 4.6337 | 7.2983 | 12.2371 |
| 90 | 8.3114 | 6.7819 | 10.4213 | 15.3344 |
| 120 | 9.9921 | 8.6363 | 12.5009 | 17.1801 |
| 150 | 11.472 | 10.0326 | 14.6942 | 19.0496 |
| 180 | 13.2223 | 11.1518 | 16.5058 | 20.2039 |
| 240 | 15.6215 | 13.6379 | 20.4738 | 22.9811 |
| 300 | 17.7944 | 16.4701 | 24.122 | 25.3469 |
| 360 | 19.3799 | 18.8045 | 27.4791 | 27.4397 |
| 420 | 21.0759 | 20.4162 | 31.1456 | 29.3505 |
| 480 | 22.0148 | 21.7544 | 35.1877 | 30.9543 |

**Table S6** Cumulative Amount diffused at different time intervals for RBC, RBC-HYD, RBC-VA-HYD and RBC-RES

| | Cumulative Amount diffused (µg/20 mL) | | | |
|---|---|---|---|---|
| Time Intervals (min) | RBC | RBC-HYD | RBC-RES | RBC-VA-HYD |
| 0 | 0 | 0 | 0 | 0 |
| 15 | 50.4257 | 46.4926 | 59.802 | 13.0499 |
| 30 | 152.4384 | 142.3759 | 196.8701 | 29.4194 |
| 60 | 256.9737 | 230.9428 | 415.5304 | 55.5704 |
| 90 | 351.9686 | 309.6174 | 655.5796 | 128.9095 |
| 120 | 432.7647 | 377.5492 | 835.1077 | 202.4025 |
| 150 | 521.5183 | 449.0152 | 993.9157 | 280.2411 |
| 180 | 615.9212 | 553.9783 | 1118.458 | 411.7327 |
| 240 | 714.1342 | 652.0004 | 1393.689 | 607.9904 |
| 300 | 828.1381 | 734.7476 | 1647.857 | 884.4655 |
| 360 | 924.4594 | 827.3236 | 1843.419 | 1137.9103 |
| 420 | 1002.991 | 919.1742 | 2066.837 | 1319.8605 |